Phase Fractions and Velocities in Multiphase Flow – Estimation using Sensor Data Fusion and Machine Learning

Andreas Lund Rasmussen [a], Kjetil Fjalestad [a], Håkon Viumdal [b,*], Ru Yan [b], Saba Mylvaganam [b], Tonni Franke Johansen [c]

[a] *EQUINOR ASA,* [b] *University College of South-Eastern Norway, Faculty of Technology, Natural Sciences and Maritime Sciences, Dept. EE, IT and Cybernetics, Kjølnes Ring 56, 3918 Porsgrunn, Norway,* [c] *SINTEF Digital*
* hakon.viumdal@usn.no

Abstract
There is a strong interest in quantifying the amount of gas and its flow rate to facilitate better control of the processes involved in many industries. There are usually many sensors monitoring these processes, both intrusive and invasive, as well as non-invasive sensors which are usually clamped on to the process pipelines in which the multiphase flow occurs. In the multiphase flow rigs at Equinor and the University of South-Eastern Norway, experiments have been performed with different combinations and velocities of the phases and multiple sensors have been logged. The data from these sensors have been used to estimate volume fractions of the phases as well as their flow rates. This paper presents the estimated results of volume fractions and velocities of selected phases, obtained by fusing data from multiple sensors that monitor density, differential pressure, temperature, and acoustic emission using machine learning (ML) algorithms. These ML algorithms use neural networks with the non-linear input-output type with Levenberg-Marquardt training and provide estimates of volume fractions and phase velocities with RMSE values in the range of 4.6 to 16 m^3/h, with the lowest RMSE for gas and the highest for multiphase flow. The total flow rate for the multiphase flow was in the range 30 to 120 m^3/h. Results are compared with ML models using data from non-invasive sensors.

1. Introduction

It is desirable to know how much oil, water, and gas each well produces in an oil and gas installation. There are many good alternatives to measure single-phase flow with high accuracy, but measuring multiphase flow is more challenging. The sand detectors used on Equinor's oil and gas installations use a piezoelectric sensor to measure the acoustic emission caused by sand production, first reported in a publication of results based on an R&D project supported by STATOIL, the forerunner to the current Equinor, (Folkestad, Mylvaganam, 1990). A multiphase flow does also generate acoustic emission. Since sand detectors are both cheap and non-intrusive Equinor is interested in using their already installed sand detectors to measure acoustic emission from the multiphase flow and fuse this data possibly with other existing measurements for enhancing the process monitoring and control. Together with other available sensors, the process industries are investigating the possibilities of determining the flow rates of individual phases as well the total flow

Related works addressing flow regimes using the multiphase rig have addressed some of the possibilities of identifying flow regimes and flow velocities, , (addressing tomographic approach by Johansen et al, 2018; related to slug modeling and control by Pedersen et al, 2017; modeling single and two-phase flow at 90^o bends in pipelines by Shoux et al 2021; and monitoring flow regime transitions with acoustic and electrostatic sensors in powder flow, Yang et al, 2019). This paper deals with some of the findings from the work done in collaboration with (Rasmussen, A.L., 2023). Some of the related work using the multiphase rig and extensive experiments, but with focus on flow regimes, is presented in the paper in SIMS 2023, (Syed Kazmi et al, 2023).

1.1 System description – Multiphase flow rig with relevant measurands

A dedicated multiphase flow rig has been in use for many years in the Equinor facilities. The system consists of feed pumps for gas, oil and water with the necessary measurements typical for flow related large scale experiments. In the current paper, the focus is only on a sensor suite consisting of the sensors, from which the data used in this study are acquired.

A P&ID of Equinor's multiphase rig is shown in Figure 1. Depending on the phase fractions and flow velocities of the different phases, the production

process can be monitored and controlled using a series of actuators placed near the reservoir (downhole) or at the entrance or exit of the separators.

The volume flow of each medium is indicated by Q_O, Q_W and Q_G with the following equations for Gas Volume Fraction (GVF), Water Liquid Ratio (WLR)

$$GVF = \frac{Q_g}{Q_{tot}}$$

$$WLR = \frac{Q_w}{Q_w + Q_o}$$

with total flow consisting of all the three phases given by

$$Q_{tot} = Q_w + Q_o + Q_g$$

These process variables are of interest in the context of measurement while drilling as well as in process monitoring during the operations of three phase flows in experimental work and oil and gas distribution. These three parameters quantifying the flows and the derived quantities WLR and GVF will be studied using AI/ML techniques with measurements from various sensors, as shown in Figure 1. This study is based on the experiments performed in the Equinor multiphase rig in Herøya, Porsgrunn in the municipality of Telemark.

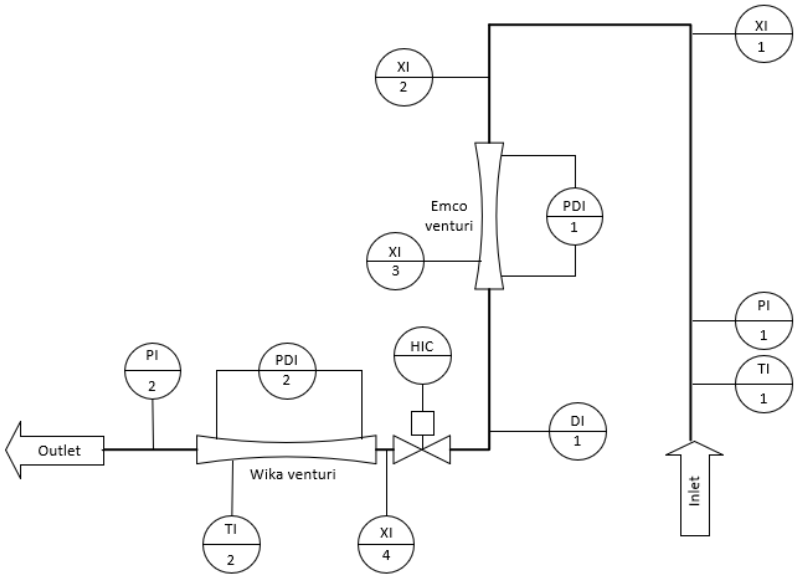

Figure 1. Simplified P&ID (Piping and Instrumentation Diagram) of the Equinor multiphase flow rig with the sensor suite selected for the current study. PDI – Differential Pressure; XI-1, XI-2, XI-3, and XI-4 – Acoustic Emission Sensors (Accelerometers). Inlet can be a single (G, O, W), two-phase (GO, GW, OW), or three-phase flow (O, G, W), with G-Gas, O-Oil, W-Water, with corresponding volume flow rates Q_G, Q_G and Q_W. These variables have been selected as input data for training the artificial neural network models: Density Krohne DI-1, dp 4m straight, Emco Venturi PDI-1, Wika Venturi PDI-2, Accelerometer *i* (XI-i) with *i* =1, ..4, Temperature Difference (TI-1) –(TI-2), Pressure Difference (PDI-1) –(PDI-2).

2. Acoustic emission sensors

The sand detector uses a piezoelectric element to detect the ultrasonic energy from sand particles colliding with the pipe wall and convert it into electrical energy. The sand production can be calculated if the flow velocity is known for the same period. The accelerometers used in the experiments for this paper operate on the same principles as those used in the sand detector. The main difference is whether the sensor detects bubbles/droplets or sand particles. A wiring diagram for a typical sensing system based on acoustic emission is shown in Figure 2.

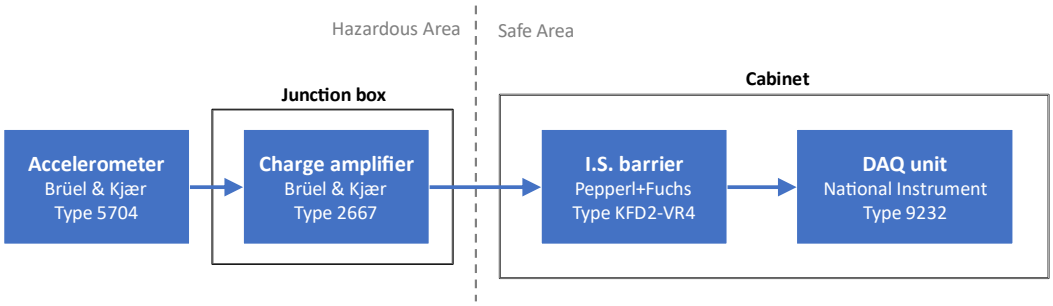

Figure 2. The main modules used in the experiment coupled together in a sensing system based on acoustic emission. I.S. barrier – Intrinsic Safety barrier, **DAQ**- **D**ata **A**c**Q**uisition Unit. The modules in the hazardous area are mounted on the pipe wall or in the vicinity of the multiphase rig, shown with the P&ID in Figure 1.

3. Data Analysis from Experiments

The level of acoustic emission in the multiphase flow varies based on process conditions. When the flow is annular at the entry of the elbow, gas bubbles tend to move to the inner curvature of the bend. Also, the GVF (Gas Volume Fraction) in a gas-liquid flow increases after a restriction in the flowline. Examples of flow restrictions are a Venturi channel or a choke valve.

The experimental data are from 20 distinct experiments involving diverse flow regimes, phase velocities and compositions. In each experiment, the flow rate of the phases are kept constant. The sampling frequency of the accelerometer is 51.2 kHz. Figure 3 presents experimental results involving combined oil and gas flow.

3.1 Analysis of the Root Mean Square (RMS) value of the acoustic emission measurements

The acoustic emission sensors give a voltage signal that can be used for further analysis. The Root Mean Square of voltages, V_{RMS}, of the samples is calculated using equation (1).

$$V_{RMS} = \sqrt{\frac{1}{N}\sum_{n=1}^{N}|V_n|^2} \qquad (1)$$

, where N represents the total number of samples in each experiment, while V_n refers to the voltage of the n^{th} sample.

Figure 3. The letters and numbers in the x-axis contain information about the experiments in dataset 1. The first two letters explain that the experiments are done on gas and oil (GO) flow. The numbers refer to the experiment number, e.g., GO01 – experiment #01 with Gas and Oil, GOC11 – Experiment #11 with Gas and Oil with Choke etc. Legends inserted in each plot indicate the parameters plotted for each experiment. The numbering of the different experiments is the same as in the paper SIMS 2023, (Syed Kazmi et al, 2023).

The V_{RMS} value is based on approximately 2000 samples from each experiment in dataset 1. Each experiment was run under steady-state conditions. The hypothesis is that the V_{RMS} value will correlate with the acoustic emission from the multiphase flow, as was reported in (Folkestad, Mylvaganam, 1990). Pure water flow seems to give low acoustic emission, while pure gas flow seems to give higher acoustic emission. However, pure oil flow seems to give much higher acoustic emission. The observed variations are possible attributed to the differences in the viscosity of the fluids. Significant adjustments in the choke position yield peaks in both total differential pressure and amplitudes of acoustic emission signals. This effect is particularly noticeable for the acoustic emission sensor 4, which is situated downstream of the choke valve, as indicated by the position of the sensor "XI-4" in Figure 1.

Pure water flow Q_w seems to generate low acoustic emission signals, and pure gas flow generates higher acoustic emission signals with gas flow Q_g and total flow Q_{tot}.

3.2 Frequency analysis of the acoustic emission sensors

Figure 4 show the dominant frequency components when increasing the gas flow when the flow contain both gas and oil. Choke valve openings are indicated by percentages in Figure 5, which shows the dominant frequency components in the lower frequency range 3kHz-5 kHz for a completely open choke valve. When the choke valve is gradually closed, there is considerable reduction in the amplitudes of these frequency components. The dominant frequency components seem to be in the range of 0 – 11 kHz for oil and water flow.

4. Preparing the dataset for the artificial neural networks

In addition to the RMS value from the acoustic emission sensors, the selected variables for training the dataset are different density, differential pressure, and temperature measurements. The sampling frequency of the accelerometers is 51.2 kHz, but the other measurements have a sampling frequency of 1 Hz. A code was therefore written to calculate one RMS value every second to get the same sampling frequency for all measurements. The acoustic emission sensors were calibrated for the background noise in the test rig before they were normalized.

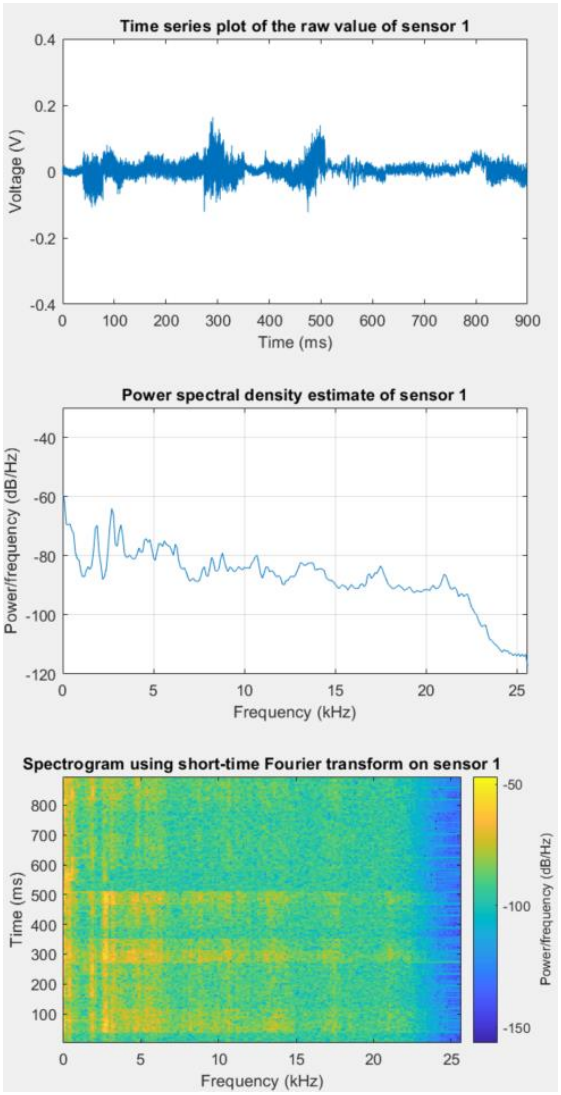

Figure 4. Results based on time series logged from Sensor 1v in GO -flow, as indicated by the position of "XI-1" in Figure 1. Spectrogram and power spectral density show incidents of increased flow in the pipe.

Both linear scaling and Z-score normalization methods were used, but Z-score gave overall best results when testing the models on other datasets. The Z-score normalization method assumes no extreme outliers is given in equation (2).

$$x' = \frac{(x-\mu)}{\sigma} \tag{2}$$

, with x representing the sample value, μ the ensemble average and σ the standard deviation.

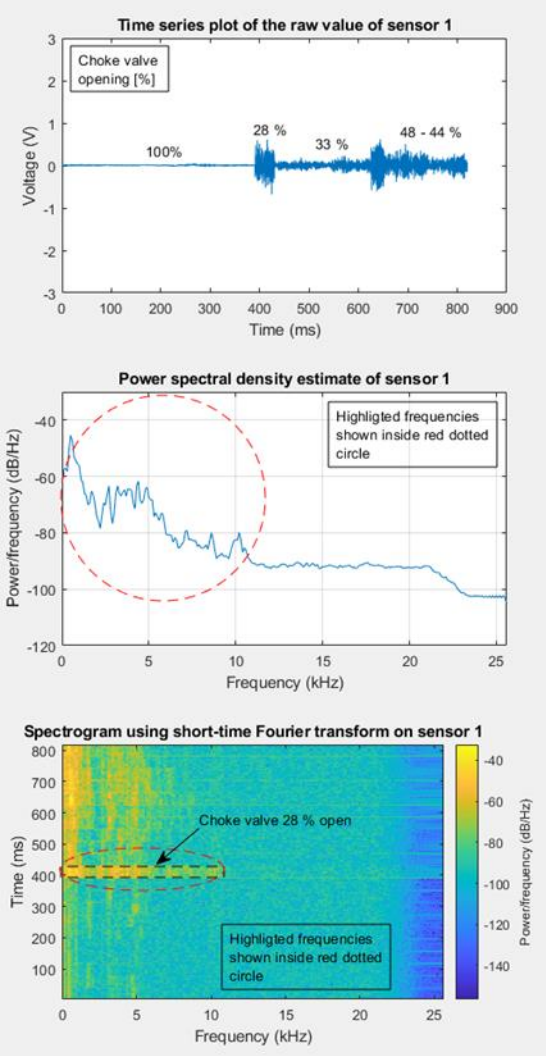

Figure 5. Results from time series logged in from Sensor 1, in OW-flow, as indicated by the position of "XI-1" in Figure 1. Both power spectral density plot and spectrogram show the effects of opening the choke valve as indicated by the circle and ellipse shown with the red dashed lines.

5. Neural network for multiphase flow estimation

The shallow nonlinear input-output network using Z-score normalization gave the best results. An example of a nonlinear input-output model is shown in Figure 6. The most important results use all four acoustic emission sensors "XI" and the differential pressure measurement over Venturi 2 "PDI-2" as inputs to the network. The sensors are all shown in the P&ID in Figure 1. There is one network each for gas, oil, water, and total flow rate. The GVF, and LWR (Water Liquid Ratio) are calculated from the flow rates.

6. Results

To illustrate the performance of the model, one set of plots comparing the actual and estimated parameters is shown in Figure 7.

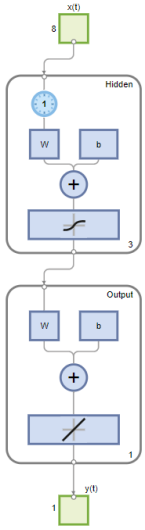

Figure 6. Nonlinear input-output neural network with one hidden layer and one output layer. This network is configured with a time delay of 1, 3 neurons in the hidden layer and 1 output in the output layer. Inputs, with reference to Figure 1: Differential pressures on two locations, acoustic emission signals (XI-I, i=1,2,3,4), density from DI-1, Difference of Temperatures TI1 and TI2. Output: gas flow rate.

7. Discussion

The frequency analysis indicates that pure oil flow gives a higher amount of acoustic emission than pure gas flow and that pure water flow gives almost zero acoustic emission. It is recommended to investigate this finding in future research since there may be a relationship between with the viscosity of the fluid, or some other variable that can be exploited. It seemed like the frequency range between 0 – 11 kHz contained the most important information. Since there was no clear conclusion in the frequency analysis all frequency components were kept avoiding the risk of filtering away important information. This decision may have been a mistake. Further investigation is needed on the frequency analysis to find out if some of the frequency components are due to noise, but also to research if there are some dominant frequency components in gas, oil, or water flow. If there is a dominant frequency component in, for instance, gas, then the amplitude of that frequency component may correlate with the gas flow rate. In the frequency analysis it was shown that there may be a relationship between frequency components around 1.7 kHz and total and water flow, but this needs to be investigated further.

The models for gas, oil, water, and total flow were trained with shallow neural networks. It is recommended to use a deep neural network in future studies to improve the results. According to MATLAB documentation, the NARX model will give more accurate predictions than the nonlinear input-output models since it uses the additional information from previous values of $y(t)$.

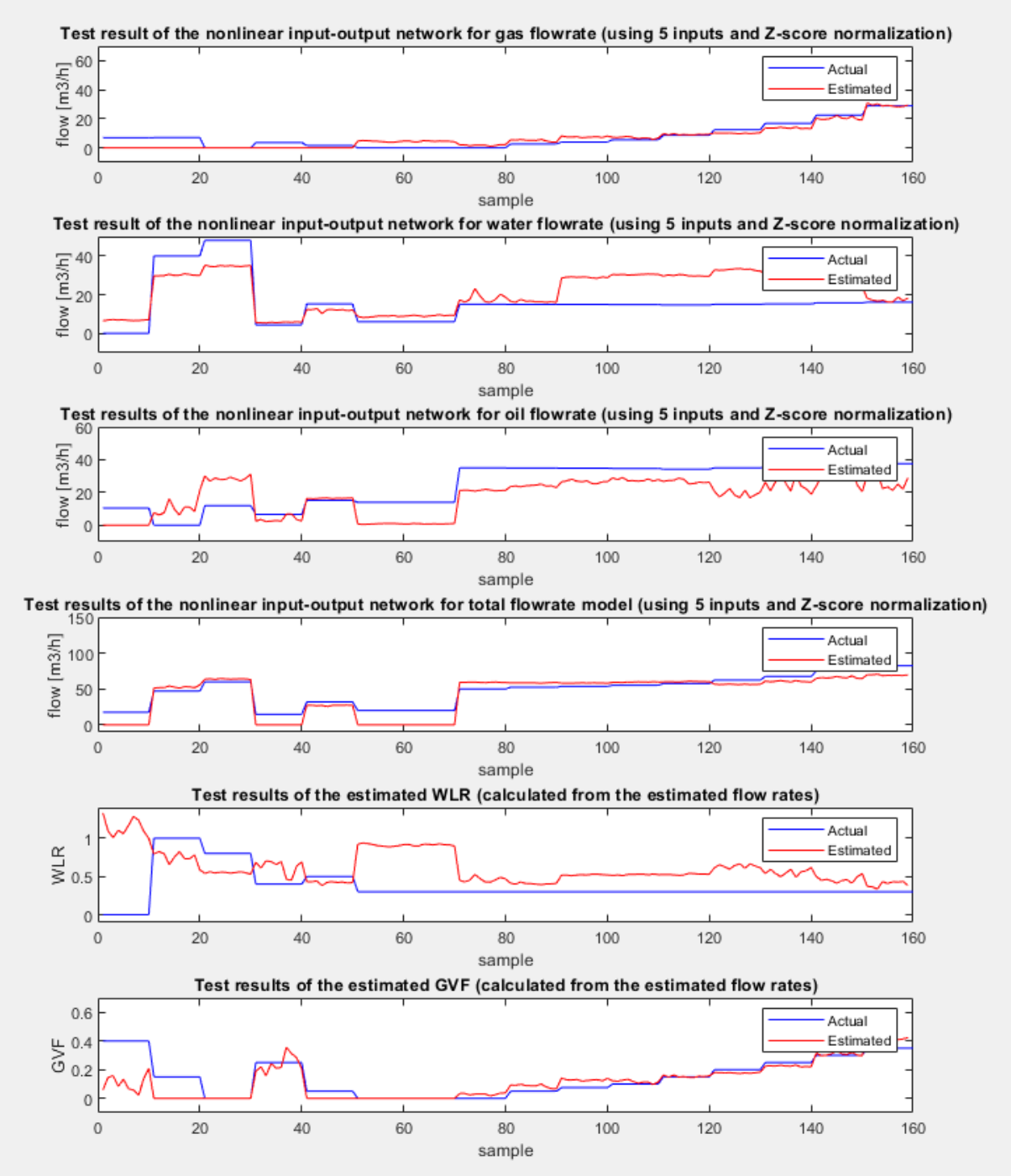

Figure 7. Comparison of estimated and actual results for WLR (Water Liquid Ratio) and GVF (Gas Volume Fraction). The 5-inputs: are: datafrom the four acoustic emission sensors (XI-I, i=1,2,3,4) and differential pressure PDI-2 over Wika Venturi meter, based on the P&ID shown in Figure 1.

In this study, it was observed that the NARX models gave the best training results, but that after closing the loop and simulating the network on the testing matrix the results were not as good as expected. The Nonlinear Input-Output models gave the best results when using the testing matrix. This network does not use the previous values of y(t) as feedback as the NARX network does. This may indicate that there is no relationship between the measured flow rate and the previously measured flow rate. The models using

7-8 inputs, gave the best results. The models with only 5 inputs, were used since they gave similar results. The models with 5 inputs are recommended since they are a more cost-effective solution with respect to execution time and resources.

There seems to be a direct relationship between the acoustic emission generated by the multiphase flow and the differential pressure, which again correlates with the total flow rate. The Root Mean Square Error (RMSE) values in Table 1 reveal that the RMSE for oil and water flow rate models are higher than for the gas flow rate model, implying less accuracy in the oil and water models which will need improvement. Since the total flow rate is the sum of oil, water, and gas flow rate, its RMSE value is higher, but the results are satisfactory. The GVF and WLR are calculated from flow rates and are therefore dependent on the accuracy of the flow rate models.

The location of the acoustic emission sensors may be vital for the results. It was shown in other studies that the GVF is increased downstream of a flow restriction like a Venturi or choke valve. Note that this is only true in the pipe just after the flow restriction and not for the whole pipe downstream the flow restriction. If this is to be interpreted as something that can be exploited in future studies or if this should be conceived as measurement noise should be investigated. If a sand detector is chosen as the acoustic emission sensor, then the location may not be ideal since it is located to best detect sand particles that collide with the outer curvature of the pipe wall, while gas bubbles seem to flow closer to the inner curvature of a 90-degree bend.

8. Conclusion

We implemented shallow nonlinear input-output neural networks for gas, oil, water, and total flows. Although the inclusion of additional sensors marginally improved accuracy, the cost-effective solution using only five measurements as input was favored due to the insignificant difference.

Equinor is keen on utilizing already installed huge number of sand detectors to measure flow velocities based on acoustic emission caused by the multiphase flow. This study suggests the potential of combining four acoustic emission sensors with differential pressure measurements over a Venturi meter to estimate multiphase flow velocities.

Shallow nonlinear input-output neural networks were created for gas, oil, water, and total flow. While including more sensors did improve the accuracy, the difference was not substantial, leading to a preference for the more cost-effective solution that only required five input measurements.

In future studies, it is recommended to use a deep neural network to improve the results to improve the results, and place greater emphasis on frequency analysis to identify dominant frequency components. The most interesting frequency range in this study appeared to be 0 – 11 kHz; however, due to the lack of a clear conclusion, all frequency components were retained throughout the study.

Table 1. An overview of the RMSE, network algorithm and configuration. The models for oil and water flow have room for improvement, while the gas and total flow models have both good accuracy and low RMSE. Dataset 1 was only available in, but dataset 2 was preferred to be used for training the data. This was due to a higher sampling rate on measurements and more available sensors.

	Network type	Training algorithm	Network configuration	RMSE
Gas flow model	Nonlinear Input-Output model	Levenberg-Marquardt	1 hidden layer with 2 neurons	4.62
Oil flow model	Nonlinear Input-Output model	Levenberg-Marquardt	1 hidden layer with 2 neurons	11.40
Water flow model	Nonlinear Input-Output model	Levenberg-Marquardt	1 hidden layer with 2 neurons	10.87
Total flow model	Nonlinear Input-Output model	Levenberg-Marquardt	1 hidden layer with 2 neurons	16.65

Acknowledgement

Many thanks to the team working with Multiphase Flow in Equinor for performing dedicated measurement campaigns to acquire the necessary data used in this study. This work was done as part of the activities of the project, SAM (SAM: Self Adapting Model-based system for Process Autonomy - SINTEF), with Equinor and SINTEF as the major partners.

References

Folkestad, T., Mylvaganam, K.S., 1990, Acoustic measurements detect sand in North Sea flow lines. Oil and Gas Journal; (USA). 88:35

Johansen, R., Østby, T.G., Dupre, A., Mylvaganam, S. , 2018, Long short-term memory neural networks for flow. 9th World Congress on Industrial Process Tomography, Bath, UK,

Pedersen, S., Durdevic, P., Yang, Z., 2017, Challenges in slug modelling and control for offshore oil and gas, International Journal of Multiphase Flow Vol. 88, pp. 270-284,

Rasmussen, A.L., 2022, Multiphase flow metering – estimation of flow velocities of component phases using multimodal sensor suite, Master Thesis, University of South -Eastern Norway

Shouxu Q., Wenyi Z., Shuang, W., Lanxin, S., Sichao, T. 2021, Numerical simulation of single and two-phase flow across 90° vertical elbows, Chemical Engineering Science, Volume 230, 116185, ISSN 0009-2509, https://doi.org/10.1016/j.ces.2020.116185.

Syed Kazmi, N., Yan, R., Mylvaganam, M., Viumdal, H., 2023, "Multimodal sensor suite for identification of flow regimes and estimation of phase fractions and velocities – Machine learning algorithms in multiphase flow metering and control, SIMS 2023

Wang,x.,Liu,Y., Xin,H.,2021,Bond strength prediction of concrete-encased steel structures using hybrid machine learning methodructures,Volume 32,Pages 2279-2292,ISSN 2352-0124,https://doi.org/10.1016/j.istruc.2021.04.018.

Yang Y., et al, 2019, Measurement and analysis of flow regimes transition by acoustic and electrostatic signals in vertical pneumatic conveying, Powder Technology, Volume 352, 2019, Pages 283-293, ISSN 0032-5910,https://doi.org/10.1016/j.powtec.2019.04.024.